11,06

Evolution of phase transitions and energy storage effect in $SrTiO_3-PbZrO_3$ solid solutions

© E.P. Smirnova, R.S. Passet, G.Yu. Sotnikova, N.V. Zaitseva, E.G. Guk, G.A. Gavrilov

Ioffe Institute,
St. Petersburg, Russia

E-mail: esmirnoffa@gmail.com

Received March 6, 2023
Revised March 6, 2023
Accepted March 11, 2023

Solid solutions $(1-x)SrTiO_{3-x}PbZrO_3$ ($x = 0.5,\ 0.6,\ 07,\ 0.8,\ 0.9$) were synthesized and their dielectric properties are investigated Measurement of dielectric hysteresis loops allowed us to obtain field dependences of the main parameters characterizing the effect of energy storage in these materials. The relationship of the obtained parameters with the evolution of the state of solid solutions from relaxors to antiferroelectrcs in this system is discussed.

Keywords: solid solutions, energy storage effect, relaxors, antiferroelectrcs.

DOI: 10.21883/PSS.2023.05.56057.30

1. Introduction

Super-fast charge/discharge process and ultra-high output power density allow to use dielectrics as the main components of state-of-the-art portable electrical and electronic equipment, including the rapidly growing battery electric vehicle industry [1–4].

It should be noted that over the last years the properties of the available dielectrics are unable any longer to satisfy the growing demand for miniaturization and integration, which promotes further studies for the purpose of development of materials with higher energy storage (storage) density and performance. Among nonorganic dielectrics, ferroelectrics with inherent maximum possible polarization P_i induced by electric field attract the most interest. Figure 1 shows a hysteresis loop for a traditional ferroelectrics — $BaTiO_3$ single-crystal, measured at 24°C in deep ferroelectric phase.

The main parameters defining the energy storage effect in a capacitor: W_{rec} and W_{loss}. The density of useful energy component Wrec stored by the capacitor when electric field W_{rec} is applied may be calculated by an area between the polarization axis and discharge curve, and loss of energy W_{loss} may be calculated by the loop area (hatched regions) [4,5]. It should be noted that, in terms of stored energy density, ferroelectrics are still inferior to ion batteries or supercapacitors [5], but hold the lead in charge/discharge rate.

However, conventional ferroelectrics demonstrate significant dielectric loss W_{loss} resulting in reduction of energy storage performance inversely proportional, in particular, to dielectric loss level. Ferroelectrics–relaxors and antiferroelectrics with perovskite structure have relatively narrow hysteresis loops in a certain temperature range and, therefore, low dielectric loss [4–7]. Taking into account potential achievement of high induced polarization levels, such materials are recognized as advantageous for the development of energy storage (storage) devices with relatively high performance [4–6].

Solid ferroelectric solutions with perovskite structure may exhibit properties considerably different from those of initial components. An example of such solid solutions is $(1-x)SrTiO_3-xPbZrO_3$ that combines, depending on x, both solid solutions–relaxors and solid solutions–antiferroelectrics [8,9]. State transformation is ob-

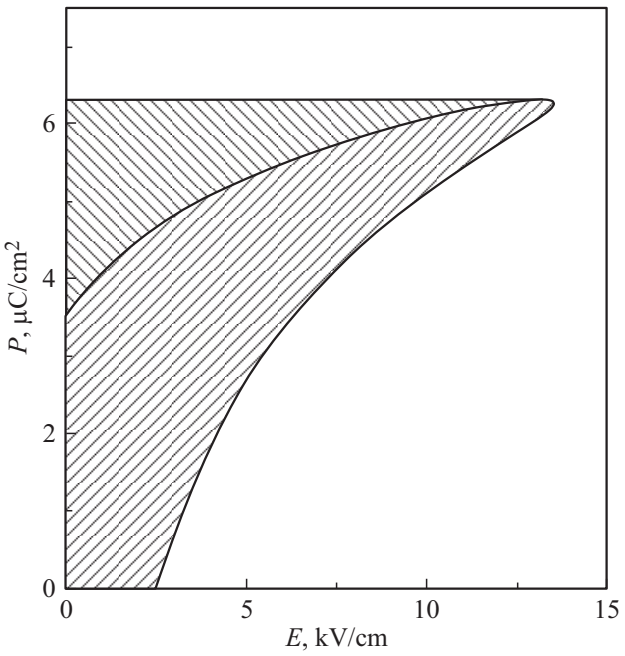

Figure 1. Typical dielectric hysteresis loop $P-E$ for a ferroelectrics. The hatched areas define the main parameters characterizing energy storage W_{rec} and energy loss W_{loss}.

served, which includes evolution from virtual $SrTiO_3$ ferroelectric followed by appearance of relaxor state (at $x \sim 0.1$) and some phase co-existence region near $x \sim 0.7$ to antiferroelectric phase at $x \geq 0.7$. This system apparently constitutes a model for investigation and comparison of the energy storage effect with phase transition evolution from relaxers to antiferroelectrics which promotes its study.

2. Experiment

Ceramic samples of $(1-x)SrTiO_3-xPbZrO_3$ system with $x = 0.5$, 0.6, 0.7, 0.8, 0.9 were synthesized using a traditional ceramic processing technique the synthesis process was conducted in lead oxide atmosphere to avoid lead loss and stoichiometry failure.

X-ray structural analysis carried out using DRON-3 X-ray diffractometer (radiation CuK_α, $\lambda = 1.54178$ Å, Ni-filter, 38 kV, 18 mA) at room temperature has shown that all samples were single-phase and had a perovskite structure. Sample density was 95–96% of the theoretical value. lattice constants of solid solutions measured using germanium as a standard varied almost linearly from $a = 3.905$ Å ($SrTiO_3$) to 4.146 Å ($PbZrO_3$) with growth of lead zirconate concentration x.

Dielectric constant spectra were measured within 10 Hz–1 MHz at room temperature using PSM 1735 analyzer. The variable electric field amplitude was 1 V/cm.

Ferroelectric/antiferroelectric loops (hysteresis loops of polarization P vs. electric field E) at 10 Hz were observed using Easy Check TF300 dielectric hysteresis loop meter (AixACCT, Germany) coupled with TRECK Model 609E-6 high voltage source. Discs with diameter 9 and thickness about 0.5 mm with burnt silver electrodes were used as measurement samples.

Properties characterizing energy storage were calculated using the known relations [10]:

$$W_{\text{rec}} = \int_{P_r}^{P_i} EdP, \tag{1}$$

$$W_{\text{st}} = \int_{0}^{P_i} EdP = W_{\text{rec}} + W_{\text{loss}}, \tag{2}$$

$$\eta = \left(\frac{W_{\text{rec}}}{W_{\text{st}}}\right) \cdot 100\%, \tag{3}$$

where P_i is the saturation polarization or maximum polarization for unsaturated loops; P_r is the residual polarization; E is applied electric field strength, W_{loss} is the density of energy scattered in the sample and defined by the area inside $P-E$ loop, W_{st} is the total energy density stored by the sample–capacity made from this material, W_{rec} is the density of stored useful energy component ($W_{\text{rec}} = W_{\text{st}}-W_{\text{loss}}$). It is apparent that W_{st} and W_{rec} are primarily determined by the maximum value at this electric field of induced polarization P_i.

3. Experimental results and discussion

Dielectric measurements of synthesized compounds supported the results obtained before during investigation of $(1-x)SrTiO_{3-x}PbZrO_3$ solid solution system [8,9]. A phase diagram fragment plotted using the obtained data and results [8,9] is shown in Figure 2.

As mentioned above, this system features ferroelectric phase transformation to relaxor state at $x \sim 0.1$ and expected morphotropic phase boundary (MPB) between the ferroelectric relaxor phase RFE and antiferroelectric phase AFE at $x \sim 0.7$. The phase diagram shows the concentration dependence of dielectric constant maximum temperature T_m at $f = 1$ KHz for compositions–relaxors and of antiferroelectric transition temperature T_{AFE} for antiferroelectric compositions ($f = 1$ KHz). The horizontal dot-and-dash line corresponds to 24°C — dielectric hysteresis loop measurement temperature. The dashed line shows the expected phase boundary between ferroelectric relaxor and antiferroelectric phases.

For composition–relaxor ($x = 0.6$), unsaturated hysteresis loops specific to temperatures higher than T_m were observed at room temperature to the left of MPB, and for compositions–aniferroelectrics ($x = 0.7$, 0.8, 0.9), typical double$P-E$ loops were observed to the right of MPB (Figure 3). $0.3SrTiO_3-0.7PbZrO_3$ solid solution features temperature dependence of the dielectric hysteresis loops type. If antiferroelectric double $P-E$ loops are observed at room temperature, then unsaturated loops inherent in ferroelectrics–relaxors are observed at 78 K [8]. This fact is reflected in the inclined line (MPB) which separates the

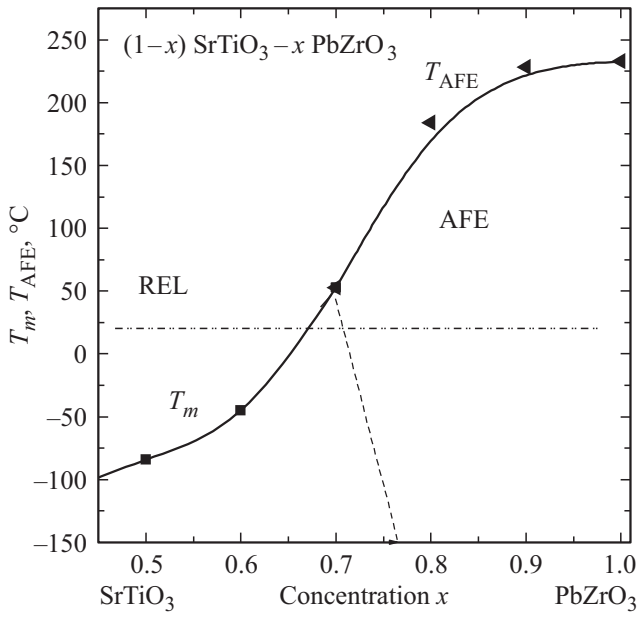

Figure 2. The phase diagram of $(1-x)SrTiO_3-xPbZrO_3$ ($0.5 \leq x \leq 1$) solid solution system obtained using dielectric and $P-E$ measurements. The dotted line corresponds to the expected MPB.

relaxor and antiferroelectric phases on the phase diagram (Figure 2).

Induced polarization P_i for solid solutions located near MPB ($x = 0.7$ and 0.8) was approximately 6 times as high as for compositions far from MPB ($x = 0.6$ and 0.9) (Figure 4). Total stored energy density W_{st} increases sharply with an increase in applied electric field E for compositions with lead zirconate concentration $x = 0.7$, 0.8 (compounds near MPB), weakly depends on the field for $x = 0.6$ and $x = 0.9$ in field range $E \leq 45$ KV/cm (Figure 5).

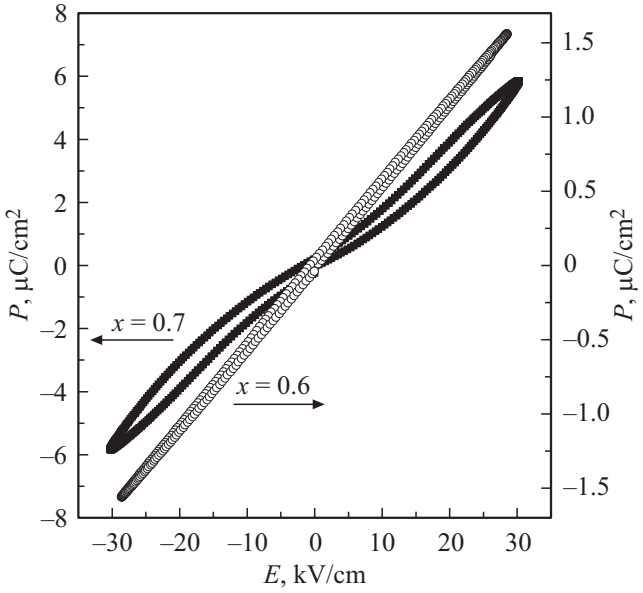

Figure 3. Hysteresis loops of relaxor ($x = 0.6$) and antiferroelectric ($x = 0.7$) measured at 24°C.

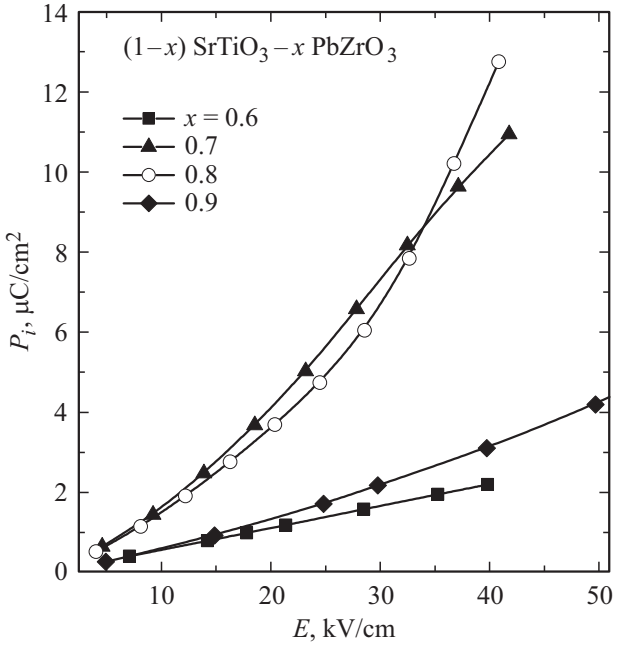

Figure 4. Dependence of the maximum induced polarization at a given field P_i on the electric field E.

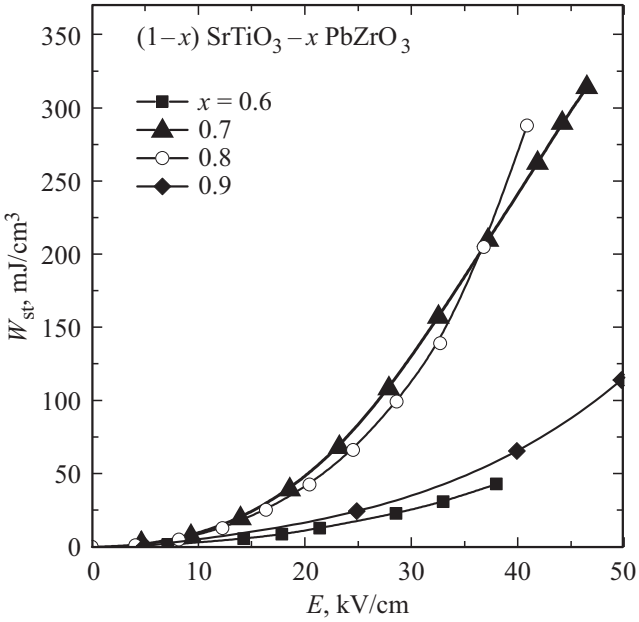

Figure 5. Dependence of the total energy density W_{st} stored by samples−capacitors made from $(1-x)SrTiO_3-xPbZrO_3$ solid solutions.

With further increase in the applied electric field ($45 < E \leq 110$ KV/cm), antiferroelectric with $x = 0.9$ also demonstrates sharp growth and achieves $W_{st} = 914$ mJ/cm^3. In this case, for all studied solid solutions, the growth rate of W_{st} is defined by both the field strength and position on the phase diagram. Dependences of the stored useful energy component density W_{rec}, i.e. density of that stored energy component that may be directly used in devices, on the filed are similar to field dependences $W_{st}(E)$ for the same compounds (Figure 6).

Energy storage efficiency is defined by coefficient $\eta = W_{rec}/W_{st}$. The efficiency decreases with field growth E, but with different rate for different lead zirconate concentrations x (Figure 7). Relaxor with $x = 0.6$ has the highest efficiency ($\eta = 95.9\%$ at $E = 7$ KV/cm). Drop of $\eta(E)$ for this compound is about 5% with an increase in E up to 40 KV/cm, which proves that this parameter is stable. Antiferroelectric ($x = 0.7$) demonstrates lower efficiency with $\eta = 92.2\%$ at $E = 7$ KV/cm and with following decrease in η by 15% at 40 KV/cm, while compositions with $x = 0.8$, 0.9 have lower efficiency and drop of η about 30% at the same field strengths. Conflict between growth W_{rec} and drop of η with an increase in the applied field E indicates that optimum combination of these parameters is required for the material used as the energy storage.

Note that the obtained W_{rec} values are typical for bulk ceramic materials and fields up to 50 KV/cm (see, for example, [6,9]). Significant values (by an order of magnitude as high as those of the bulk samples) were observed only in thin films and in fields up to hundreds of KV/cm, for example, [6,10].

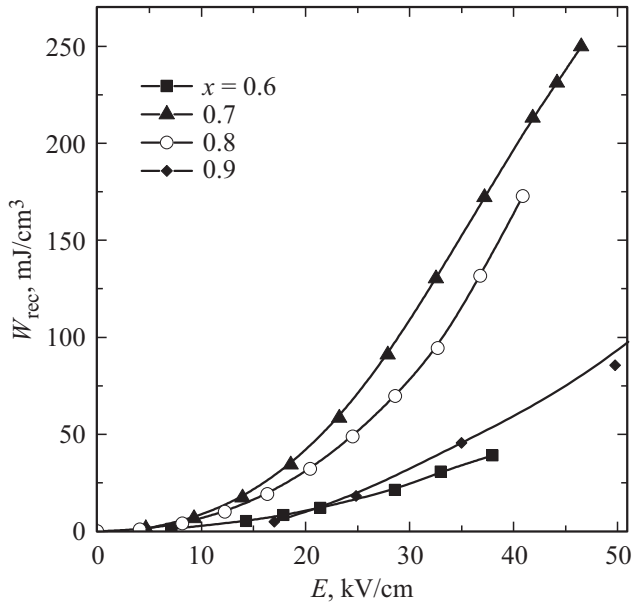

Figure 6. Dependence of W_{rec} on electric field E for $(1-x)SrTiO_3-xPbZrO_3$ solid solutions.

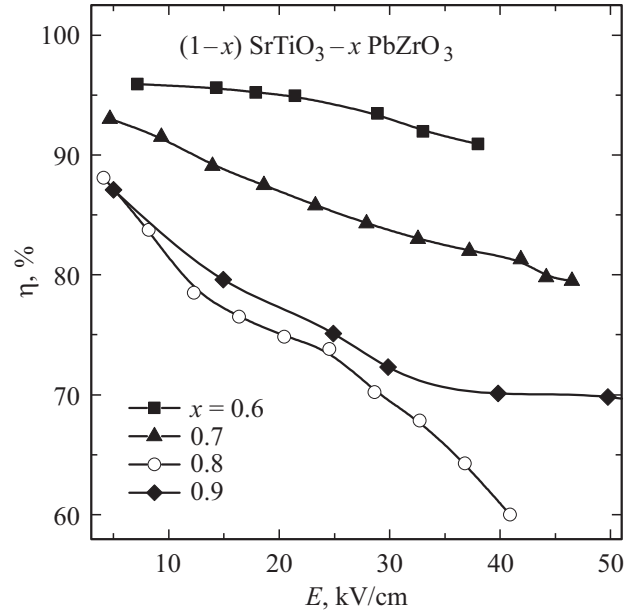

Figure 7. Energy storage efficiency coefficient η depending on electric field E for $(1-x)SrTiO_3-xPbZrO_3$ solid solutions.

Solid solutions based on lead zirconate are known to have morphotropic phase boundary MPB [11]. At MPB, co-existence and instability of phases inherent in the initial components makes the structure especially sensitive to environmental impacts such as electric field. These are compositions lying on MPB that have extraordinary electrical and mechanical properties and are widely used as piezoelectric materials for various applications, including ultrasonic transducers, sensors and actuators. The nature of the extraordinary properties near MPB is still underway. The co-existence of two phases (rhombohedral and tetragonal) facilitates polarization re-orientation resulting in strong piezoelectric effect [11]. The next assumption associated the effect with the transition from rhombohedral to tetragonal phase induced by electric field where the total polarization is drawn towards [001] [12]. After discovery of the monoclinic phase at MPB, the effect was explained by polarization rotation from polar directions towards the applied electric field provided that one (or more) monoclinic phase is present [13]. Monoclinic phase is addressed in this case as a kind of structural low-symmetrical bridge between the highly-symmetrical rhombohedral and tetragonal phases that facilitates polarization re-orientation. This model, however, has not been accepted completely. There is data that monoclinic phases really represent the co-existence of rhombohedral and tetragonal phase microdomens [14–16].

In case of relaxor-based solid solutions with MPB, the high sensitivity of the medium to environmental impacts is caused by the existence of polar regions (PNR) near MPB. PNR-related dynamic nature of MPB when the soft mode for lead magnesium niobate — lead titanate PMN — 0.32PT located on MPB behaves almost identically to that of the pure lead magnesium niobate PMN that was experimentally supported, for example, during the study of inelastic neutron scattering in the temperature range 100–600 K [17]. Also of interest is the proof obtained in [18] for the dynamic nature of MPB when acoustic attenuation peaks are detected at Burns temperature for $(1-x)$ PFW — x PT $(0.25 \leq x \leq 0.35)$ solid solutions located on MPB.

$(1-x)SrTiO_3-xPbZrO_3$ systems belongs to a family of numerous solid solutions based on lead zirconate and demonstrates the boundary between ferroelectric relaxor and antiferroelectric phases at $x \approx 0.7$. There are reasons to suggest that, like solid solutions with MPB based on traditional relaxors, MPB of this system is caused by the co-existence and frustration of polar nanoregions (PNR) on the relaxor phase and antiferroelectric clusters side. Such type of morphotropic phase boundary has not observed until now. To prove this assumption, detail study of MPB of this system are required, including temperature dependences of inelastic neutron scattering and high resolution X-ray diffraction.

4. Conclusions

Measurements of W_{st}, W_{rec}, η characterizing energy storage in capacitors based on $(1-x)SrTiO_3-xPbZrO_3$ solid solutions have been carried out. This system features transformation from ferroelectrics–relaxors $(x \approx 0.1)$ through the intermediate phase (morphotropic phase boundary) at $x \approx 0.7$ to antiferroelectric phase $(x > 0.7)$ depending on lead zirconate concentration x at room temperature. Maximum W_{st} and W_{rec} values at energy transformation efficiency η higher than 90% have been obtained for a compound $(x = 0.7)$ located on the morphotropic phase boundary. Co-existence of polar nanoregions and antiferroelectric clusters near MPB was delete been suggested

and causes the increase in the energy storage effect compared with the relaxor ($x = 0.6$) and antiferroelectrics ($x = 0.8,\ 0.9$).

Acknowledgments

The authors are grateful to A.V.Sotnikov for fruitful discussions and recommendations.

Conflict of interest

The authors declare that they have no conflict of interest.

References

[1] Prateek, V.K. Thakur, R.K. Gupta. Chem. Rev. **116**, *7*, 4260 (2016).
[2] Z. Yao, Z. Song, H. Hao, Z. Yu, M. Cao, S. Zhang, M.T. Lanagan, H. Liu. Adv. Mater. **29**, *20*, 1601727 (2017).
[3] Q. Li, F.-Z. Yao, Y. Liu, G. Zhang, H. Wang, Q. Wang. Annu. Rev. Mater. Res. **48**, 219 (2018).
[4] H. Palneedi, M. Peddigari, G.-T. Hwang, D.-Y. Jeong, J. Ryu. Adv. Funct. Mater. **28**, *42*, 1803665 (2018).
[5] Z. Liu, T. Lu, J. Ye, G. Wang, X. Dong, R. Withers, Y. Liu. Adv. Mater. Technol. **3**, *9*, 1800111 (2018).
[6] P. Zhao, Z. Cai, L. Wu, Ch. Zhu, L. Li, X. Wang. J. Adv. Ceram. **10**, *6*, 1153 (2021).
[7] S. Pal, P.P. Biswas, M. Rath, M.S.R. Rao, M. Miryala, M. Murakami, P. Murugavel. J. Phys. D **54**, *4*, 045302 (2021).
[8] E.P. Smirnova, A.V. Sotnikov, M. Weihnacht, W. Häßler, V.V. Lemanov. J. Eur. Ceram. Soc. **21**, 1341 (2001).
[9] E.P. Smirnova, A.V. Sotnikov, O.E. Kvyatkovskii, M. Weihnacht, V.V. Lemanov. J. Appl. Phys. 101, 084117 (2007).
[10] Z. Liu, T. Lu, J. Ye, G. Wang, X. Dong, R. Withers, Y. Liu. Adv. Mater. Technol. **3**, *9*, 1800111 (2018).
[11] B. Jaffe, W.R. Cook, H. Jaffe. Piezoelectric Ceramics. Academic Press, London (1971). 317 p.
[12] S.E. Park, T.R. Shrout. J. Appl. Phys., **82**, *4*, 1804 (1997).
[13] M. Davis. PhD Thesis. EPFL (2006).
[14] A.G. Khachaturyan, S.M. Shapiro, S. Semenovskaya. Phys. Rev. B **43**, *13*, 10832 (1991).
[15] Y.M. Jin, Y.U. Wang, A.G. Khachaturyan. J. Appl. Phys., **94**, *5*, 3629 (2003).
[16] Y.U. Wang. Phys. Rev. B **73**, *1*, 014113 (2006).
[17] H. Cao, C. Stock, G. Xu, P.M. Gehring, J. Li, D. Viehland. Phys. Rev. B, **78**, *10*, 104103 (2008).
[18] E. Smirnova, A. Sotnikov, M. Shevelko, N. Zaitseva, H. Schmidt. J. Mater. Sci. **56**, *7*, 4753 (2021).

Translated by E.Ilyinskaya